A Novel DOTA-α-Melanocyte–Stimulating Hormone Analog for Metastatic Melanoma Diagnosis

Sylvie Froidevaux, PhD; Martine Calame-Christe, PhD; Heidi Tanner; Lazar Sumanovski, BSc; and Alex N. Eberle, PhD

Laboratory of Endocrinology, Department of Research, University Hospital and University Children's Hospital, Basel, Switzerland

Scintigraphic imaging of metastatic melanoma lesions requires highly tumor-specific radiolabeled compounds. Because both melanotic and amelanotic melanomas overexpress receptors for α-melanocyte–stimulating hormone (α-MSH; receptor name: melanocortin type 1 receptor, or MC1R), radiolabeled α-MSH analogs are potential candidates for melanoma diagnosis. The aim of this study was to develop a melanoma-selective radiolabeled α-MSH analog suitable for melanoma diagnosis. **Methods:** The very potent α-MSH analog [Nle^4, D-Phe^7]-α-MSH (NDP-MSH) and a newly designed α-MSH octapeptide analog, [βAla^3, Nle^4, Asp^5, D-Phe^7, Lys^{10}]-α-MSH$_{3–10}$ (MSH$_{oct}$), were conjugated to the metal chelator 1,4,7,10-tetraazacyclododecane-1,4,7,10-tetraacetic acid (DOTA) to enable radiometal incorporation. The resulting DOTA conjugates were evaluated in vitro for their MC1R-binding affinity and melanogenic activity in isolated mouse B16F1 cells and in vivo for their biodistribution in mouse models of primary and metastatic melanoma after labeling with ^{111}In. **Results:** DOTA-MSH$_{oct}$ was shown to bind with high affinity (inhibitory concentration of 50% [IC$_{50}$] = 9.21 nmol/L) to the MC1R, although with lower potency than does DOTA-NDP-MSH (IC$_{50}$ = 0.25 nmol/L). In B16F1 melanoma-bearing mice, both ^{111}In-DOTA-NDP-MSH and ^{111}In-DOTA-MSH$_{oct}$ exhibited high MC1R-mediated uptake by melanoma, which differed by a factor of only 1.5 at 4 h after injection. The main route of excretion for both radioconjugates was the kidneys, whereby ^{111}In-DOTA-MSH$_{oct}$ led to somewhat higher kidney values than did ^{111}In-DOTA-NDP-MSH. In contrast, the latter was much more poorly cleared from other nonmalignant tissues, including bone, the most radiosensitive organ. Therefore, ^{111}In-DOTA-MSH$_{oct}$ displayed higher uptake ratios of tumor to nontarget tissue (e.g., tumor-to-bone ratio 4 h after injection was 4.9 for ^{111}In-DOTA-NDP-MSH and 53.9 for ^{111}In-DOTA-MSH$_{oct}$). Lung and liver melanoma metastases could easily be visualized on tissue section autoradiographs after injection of ^{111}In-DOTA-MSH$_{oct}$. Radio–reversed-phase high-performance liquid chromatography analysis of urine samples revealed that most ^{111}In-DOTA-MSH$_{oct}$ is excreted intact 4 h after injection, indicating good in vivo stability. **Conclusion:** ^{111}In-DOTA-MSH$_{oct}$ exhibits more favorable overall performance than does ^{111}In-DOTA-NDP-MSH in murine models of primary and metastatic melanoma, making it a promising melanoma imaging agent.

Key Words: melanoma imaging; melanocortin type 1 receptor; α-melanocyte–stimulating hormone; DOTA; scintigraphy

J Nucl Med 2002; 43:1699–1706

The incidence and mortality rate of cutaneous melanoma are increasing in the United States, as in most countries, and this skin cancer is currently the most common malignancy among young adults (*1*). Unless tumors are detected early and adequate surgery can be performed, the prognosis is poor. This has motivated several investigations aiming at developing melanoma-specific radiopharmaceuticals for imaging and staging but also with the intention of using them for internal radiotherapy. They include radiolabeled monoclonal antibodies or antibody fragments directed against specific melanoma cell epitopes (*2–5*), as well as thiourea (*6*), which accumulates preferentially in melanin-producing melanoma by virtue of its affinity for the pigment. So far, their clinical impact has been low because of the lack of specificity due, in part, to the presence of individual tumor variants and the high occurrence of amelanotic metastases.

Another approach was based on the finding that isolated melanoma cells and melanoma tissues overexpress high-affinity α-melanocyte–stimulating hormone (α-MSH) receptors (melanocortin type 1 receptor, or MC1R; reviewed in (*7*)) and the consequent possibility of using radiolabeled α-MSH analogs as imaging tools. Compared with the use of antibodies or antibody fragments, the use of small peptides as vectors offers several advantages such as negligible immunogenicity, improved tumor penetration, and faster blood clearance. The suitability of peptides as diagnostic tools is well illustrated by the successful development of the peptide chelator conjugate ^{111}In-diethylenetriaminepentaacetic acid (DTPA) octreotide, which is routinely used in the clinic to visualize somatostatin-receptor–positive malignancies (*7*). Preclinical and clinical trials based on α-MSH analogs labeled with either ^{18}F through attachment of *N*-succinimidyl-4-^{18}F-fluorobenzoate or ^{111}In after conjugation to the

Received Dec. 26, 2001; revision accepted Aug. 8, 2002.

For correspondence or reprints contact: Sylvie Froidevaux, PhD, Department of Research, Kantonsspital Basel, Hebelstrasse 20, CH-4031 Basel, Switzerland.

E-mail: sylvie.froidevaux@unibas.ch

metal chelator DTPA showed that melanoma tumors can be targeted and visualized with radiolabeled α-MSH (reviewed in (*8*)). However, high nonspecific accumulation of these compounds in tissues, such as liver (*9*), known to be common sites of distant melanoma metastases prevented further clinical development of DTPA-α-MSH compounds. Recently, a Tc^{2+}-labeled α-MSH analog incorporating the radiometal directly into the peptide molecule was reported to exhibit favorable properties for melanoma imaging in a mouse model (*10*).

An α-MSH analog that can hold not only 2^+-charged radiometals but also 3^+-charged radiometals would greatly increase the range of application for diagnosis and therapy of melanoma because many radioactive isotopes of 3^+-charged radiometals are used—or are of potential use—in nuclear oncology. In the field of radiotherapy, such a radiopeptide is likely to augment the efficacy of the treatment by making possible the selection of the radionuclide having the physical characteristics matching the biologic characteristics of the tumor, for example, a low–β-energy emitter for micrometastasis. To produce this pluripotent α-MSH analog, the selection of the metal chelator is critical. 1,4,7,10-tetraazacyclododecane-1,4,7,10-tetraacetic acid (DOTA) is an interesting candidate because it was shown to strongly incorporate a multitude of 2^+- or 3^+-charged radiometals (*11*,*12*) and to compare favorably with DTPA with respect to the tumor-targeting performance of radiolabeled peptides in animal models (*13*,*14*) and in patients (*15*). Here, we report the development and biologic characteristics of a novel DOTA-α-MSH analog suitable for melanoma tumor targeting.

MATERIALS AND METHODS

Peptides and Radioligands

α-MSH was a gift from Novartis (Basel, Switzerland). The α-MSH analogs [βAla^3, Nle^4, Asp^5, D-Phe^7, Lys^{10}]-α-$MSH_{3–10}$ (MSH_{oct}) and [Nle^4, D-Phe^7]-α-MSH (NDP-MSH) were synthesized in our laboratory using the usual continuous flow technology and Fmoc (9-fluorenylmethoxycarbonyl) strategy. For conjugation of the peptide to DOTA, 4,7,10-tricarboxymethyl-tert-butyl ester 1,4,7,10-tetraazacyclododecane-1-acetate (*16*) (56.4 mg, 80.4 μmol), 0-[7-azabenzotriazole-1-yl]-1,1,3,3-tetramethyluronium hexafluorophosphate (36.7 mg, 96.4 μmol), and *N*,*N*′-diisopropyl ethylamine (33 μL, 192.9 μmol) were preincubated in *N*,*N*-dimethylformamide (1.3 mL) for 10 min before addition of peptide resin (100 mg). The reaction mixture was stirred for 18 h, and the resin was washed 4 times with *N*,*N*-dimethylformamide, 3 times with dichloromethane, 2 times with methanol, and 3 times with isopropanol and then evaporated until complete desiccation. Deprotection and cleavage from the resin were performed by dissolving 100 mg DOTA peptide resin in a deprotection mixture containing 4.6 mL trifluoroacetic acid (TFA), 0.3 mL thioanisole, 0.1 mL water, and 0.01 mL 1,2-ethanedithiol. After being stirred for 4 h, DOTA peptide was precipitated with ice-cold diethyl ether and resuspended in 10% acetic acid before purification by reversed-phase high-performance liquid chromatography (RP-HPLC). The major peak was collected and analyzed by electrospray ionization mass spectrometry.

The radiometal ^{111}In was incorporated into DOTA peptides by the addition of $^{111}InCl_3$ (185 MBq, Mallinckrodt, Petten, The Netherlands) to DOTA peptide (10 μg, 7 nmol) dissolved in 115 μL acetate buffer (0.4 mol/L, pH 5) containing gentisic acid (4.2 mg, 27 μmol). After a 25-min incubation at 95°C, the purity of the resulting radioligand was assessed by RP-HPLC on a 1050 chromatography system (Hewlett-Packard Co., Palo Alto, CA) connected to a flow-through LB506C1 γ-detector (Berthold, Bundoora, Victoria, Australia) and a C18-RP column (model 218TP54; Grace Vydac, Hesperia, CA); the conditions were as follows: eluent A = 0.1% TFA in water; eluent B = acetonitrile; gradient = 95% A at 0–5 min, 95%–0% A at 5–10 min, 0% A at 10–15 min, and 0%–95% A at 15–20 min; and flow = 0.75 mL/min. When necessary, the radiolabeled DOTA peptide was purified on a small reversed-phase cartridge (Sep-Pak C18; Waters Corp., Milford, MA) using ethanol as solvent. The ethanol fraction containing the purified radiopeptide was then evaporated under argon. The specific activity of the radioligands was always greater than 37 GBq/μmol. Iodination of NDP-MSH was performed as previously described using the Enzymobead reagent (Bio-Rad Laboratories Inc., Hercules, CA), consisting of immobilized lactoperoxidase and glucose oxidase (*17*).

Cell Culture

The mouse melanoma cell line B16F1 (*18*) was cultured in modified Eagle's medium (MEM) supplemented with 10% heat-inactivated fetal calf serum, 2 mmol/L L-glutamine, 1% nonessential amino acids, 1% vitamin solution, 50 U/mL penicillin, and 50 μg/mL streptomycin (all from Gibco, Paisley, U.K.) at 37°C in a humidified atmosphere of 95% air and 5% CO_2. For expansion or experiments, the cells were detached with 0.02% EDTA in phosphate-buffered saline (150 mmol/L, pH 7.2–7.4).

In Vitro Assays

Competitive binding experiments were performed by incubating MC1R-expressing B16F1 cells (1–2 million) with the radioligand ^{125}I-NDP-MSH (200,000 cpm) and a series of dilutions of competitor peptides (from 1×10^{-6} to 1×10^{-12} mol/L) in binding medium consisting of MEM with Earle's salts (Gibco) supplemented with 0.2% bovine serum albumin and 1 mmol/L 1,10-phenanthroline (Merck, Darmstadt, Germany). After 3 h of incubation at 15°C, unbound radioactivity was removed by centrifugation of cells through a layer of silicon oil (AR 20/AR 200, 1 vol/1 vol; density, 1,013 kg/m^3; Wacker-Chemie, Munich, Germany). The cell-associated radioactivity was then counted in an LKB MultiGamma counter (Packard BioScience Co., Meriden, CT), and inhibitory concentration of 50% (IC_{50}) was calculated using Prism software (GraphPad Software, San Diego, CA).

The biologic activity of the α-MSH derivatives was assessed with an in situ melanin assay. B16F1 cells (2,500 per well, 100 μL) were distributed in cell culture flat-bottom 96-well plates in medium consisting of MEM without phenol red and supplemented with 10% heat-inactivated fetal calf serum, 2 mmol/L L-glutamine, 1% nonessential amino acids, 1% vitamin solution, 50 U/mL penicillin, 50 μg/mL streptomycin, and 0.31 mmol/L L-tyrosine (all from Gibco). After overnight incubation in a cell incubator at 37°C, serial concentrations (from 1×10^{-8} to 1×10^{-12}, 100 μL) of α-MSH derivatives were added and incubation was prolonged for an additional 72 h. Melanin production was then monitored by

measurement of the absorbance at 310 nm in a microplate reader (Spectra MAX 190; Molecular Devices, Menlo Park, CA).

Biodistribution and Stability of Radioligands After Kidney Excretion

All animal experiments were performed in compliance with the Swiss regulation for animal treatment.

Female B6D2F1 mice (C57BL/6 × DBA/2 F1 hybrids, breeding pairs; IFFA-CREDO, l'Arbresle, France) received subcutaneous implants of 0.5 million B16F1 cells. One week later (tumor size range, 4.9–1,002 mg), 200 μL of 185 kBq radioligand diluted in NaCl and 0.1% bovine serum albumin, pH 7.5, were injected into the lateral tail vein. For determination of nonspecific uptake, 50 μg α-MSH were coinjected with the radioligand. The animals were sacrificed at the indicated times (4, 24, or 48 h). Organs and tissues of interest were dissected and rinsed of excess blood, weighed, and assayed for radioactivity in a γ-counter. The percentage injected dose per gram (%ID/g) was calculated for each tissue. The total counts injected per animal were calculated by extrapolation from counts of a standard taken from the injected solution for each animal.

As part of the biodistribution experiments, samples of urine were collected from melanoma-bearing mice 4 h after injection of 185 kBq ^{111}In-DOTA peptide and kept frozen at −80°C until use. Urine (1 vol) was mixed with methanol (2 vol) to precipitate the proteins and was then analyzed by RP-HPLC on a PU-980 chromatography system (Jasco Inc., Easton, MD) connected to a Radiomatic 500TR LB506C1 γ-detector (Packard BioScience) and a Spherisorb ODS2/5 μm column (Waters, Milford, MA) under the following conditions: eluent A = 0.1% TFA in water; eluent B = 0.1% TFA:30% water:70% acetonitrile; gradient = 85% A at 0–5 min, 85%–53% A at 5–10 min, 53%–45% A at 10–15 min, 45%–42% A at 15–18 min, 42%–0% A at 18–24 min, 0% A at 24–29 min, and 0%–85% A at 29–30 min; and flow = 1.0 mL/min.

Autoradiography

Mice bearing a primary melanoma were generated as described for the biodistribution experiments. Metastases were induced in B6D2F1 mice by intravenous injection of 2–5 × 10^4 B16F1 cells exposed for 2 d to 10–100 U/mL interferon-γ (Pharmingen, San Diego, CA). The cells were pretreated with interferon-γ to increase their metastatic potential of B16F1 cells. One week later (primary melanoma) or 3–4 wk later (metastatic melanoma), the mice were injected with 555–740 kBq radioligand 4 h before sacrifice; then, tissues of interest were removed and immediately fixed in isopentane cooled in liquid nitrogen. Frozen sections (100 μm thick) were then cut using an HM 560 microtome (Microm, Walldorf, Germany), refrigerated at −25°C, and transferred onto glass slides precooled on dry ice. The tissue sections were then placed in a lyophilization device (LDC-1M; Kühner, Birsfelden, Switzerland) and were evaporated overnight until complete dryness before exposure to a storage phosphor plate (Molecular Dynamics, Sunnyvale, CA) for 1–2 d. The phosphor plate was then scanned with a PhosphorImager using ImageQuant (Molecular Dynamics) to obtain digital autoradiographs, which were further processed with Photoshop 5.0 (Adobe Systems Inc., San Jose, CA). With this method, possible artifacts due to diffusion of ^{111}In-DOTA-MSH_{oct} (or its metabolites) after tissue removal were avoided because the tissue remained frozen during the entire procedure and the sections were exposed dehydrated to the phosphor plate. After autoradiography, dehydrated tissue sections were scanned (model EU-35; Seiko Epson Corp., Magano, Japan), processed using Photoshop 5.0, and superimposed to the autoradiographs.

Statistical Analysis

Unless otherwise stated, results are expressed as mean ± SEM. Statistical evaluation was performed using the unpaired Student *t* test. A probability value less than 0.05 was considered to indicate a statistically significant difference.

RESULTS

Synthesis of DOTA-NDP-MSH and DOTA-MSH_{oct}

The synthesis of MSH_{oct} and NDP-MSH and their conjugation to the metal chelator DOTA (Fig. 1) was performed as described in the Materials and Methods. DOTA-MSH_{oct} was obtained at >99% purity and at a 66.6% overall yield (after RP-HPLC purification). Mass spectrometry confirmed the expected molecular weight for DOTA-MSH_{oct} (experimental = 1,457.4 g/mol, calculated = 1,457.7 g/mol) and DOTA-NDP-MSH (experimental = 1,991.7 g/mol, calculated = 1,991.2 g/mol).

Receptor Binding and Biologic Activity

The MC1R binding affinity of DOTA-NDP-MSH, MSH_{oct}, and its DOTA conjugate were assessed by a competition binding experiment with B16F1 cells. Table 1 lists their IC_{50} as well as that of the natural ligand α-MSH, included as a control. MSH_{oct} exhibited a high receptor affinity similar to that found with the native peptide α-MSH. As expected, its attachment to DOTA decreased its binding potency (7.4 times), but the conjugate retained a favorable (low-nanomolar range) IC_{50}. DOTA-NDP-MSH displayed the highest MC1R binding affinity. Furthermore, MSH_{oct} and DOTA-MSH_{oct} displayed good α-MSH agonist activity as demonstrated by their induction of melanin synthesis by B16F1 cells at a dose matching their IC_{50}s (Table 1). Thus, DOTA-MSH_{oct} is an α-MSH agonist with high affinity to MC1R but, in vitro, is less potent than DOTA-NDP-MSH.

Biodistribution in Melanoma-Bearing Mice

Table 2 presents the tissue distribution 4, 24, and 48 h after injection of ^{111}In-DOTA-NDP-MSH and ^{111}In-DOTA-MSH_{oct} into mice implanted with B16F1 cells. Both radioligands accumulated in the tumor to reach a maximum of 4.31 %ID/g (^{111}In-DOTA-MSH_{oct}) and 6.32% (^{111}In-DOTA-NDP-MSH) at the earliest time tested (4 h). Coinjection of an excess of α-MSH to block the MC1Rs reduced the 4-h tumor uptake by an average of 86%, indicating that both radioligands are taken up in the melanoma by a receptor-mediated process. Blood clearance of ^{111}In-DOTA-MSH_{oct} was rapid; 4 h after injection, blood-associated radioactivity was as little as 0.03 %ID/g. This was associated with a fast elimination of radioactivity from MC1R-

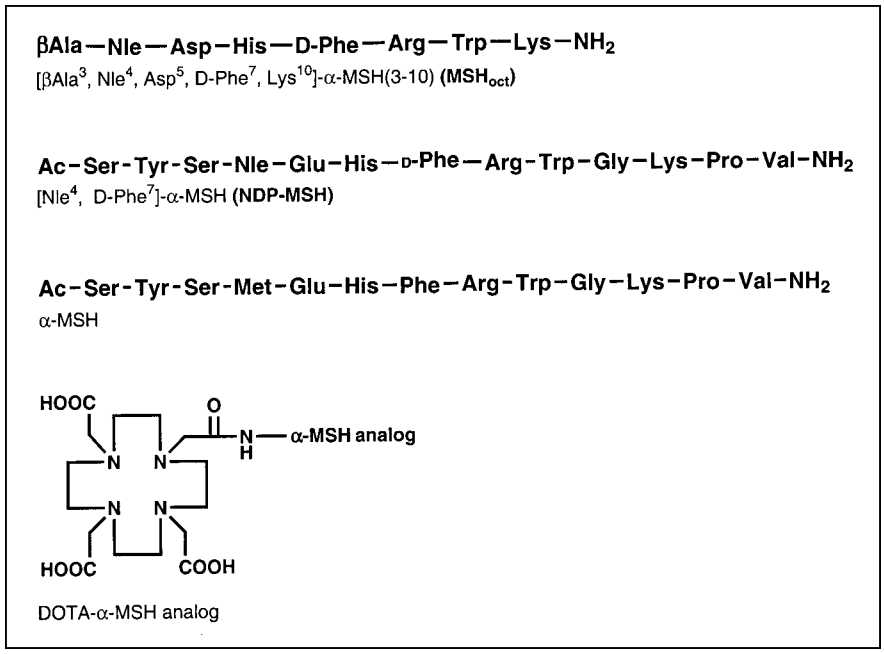

FIGURE 1. Structure of MSH_{oct}, NDP-MSH, α-MSH, and DOTA-α-MSH analog.

negative tissues, including those that are involved in the excretion process, such as liver and small intestine, and those that are highly radiosensitive, such as bone. The only exception was kidney, which showed persistent radioactivity retention, starting from 13.5 %ID/g at 4 h after injection and still representing 4.89 %ID/g 44 h later. Blockage of MC1R with α-MSH could not reduce kidney uptake, demonstrating that it is MC1R independent. In contrast, at the times tested, ^{111}In-DOTA-NDP-MSH accumulated in higher amounts in all nonmalignant tissues except kidney, particularly in bone (1.29 %ID/g, 4 h after injection) and, to a lesser extent, in muscle, skin, and spleen.

Accordingly, the ratios of radioactivity in melanoma tissue to radioactivity in nontarget tissues 4 h after injection were much greater for ^{111}In-DOTA-MSH_{oct}, with values of at least 10 and often greater than 100, except for kidney, which had a ratio of 0.3 (Fig. 2). Most notably, the 4-h tumor-to-bone and tumor-to-muscle uptake ratios for ^{111}In-DOTA-MSH_{oct} were, respectively, 11 times and 22 times greater.

In summary, ^{111}In-DOTA-MSH_{oct} displayed more favorable overall biodistribution than did ^{111}In-DOTA-NDP-MSH in melanoma-bearing mice, as demonstrated by high tumor retention and low or very low uptake in all nontarget tissues (except kidney).

TABLE 1
MC1R Affinity and Biologic Activity of α-MSH Analogs

MSH analogs	IC_{50}* (nmol/L)	EC_{50}† (pmol/L)
α-MSH	1.19 ± 0.27‡	66 ± 16.7‡
DOTA-NDP-MSH	0.25 ± 0.02‡	ND
MSH_{oct}	1.25 ± 0.08‡	35.4 ± 9.1‡
DOTA-MSH_{oct}	9.21 ± 1.27	354 ± 100

*MC1R affinity of α-MSH analogs was assessed by competition binding experiments with B16F1 cells and ^{125}I-NDP-MSH as radioligand (n = 3).

†Biologic activity of α-MSH analogs was determined in melanin assay with B16F1 cells, and results are expressed as concentration inducing half-maximal response (EC_{50}, n = 2–9).

‡$P < 0.01$ vs. DOTA-MSH_{oct}.

ND = not determined.

Data are mean ± SEM.

Autoradiography of Malignant and Normal Tissues

For the most favorable DOTA-α-MSH analog, that is, ^{111}In-DOTA-MSH_{oct}, the distribution of radioactivity within the tissues of interest (primarily tumor, liver, and kidney) was further examined using tissue section autoradiography (Fig. 3). The tumor was intentionally collected along with its surrounding skin tissue to assess selectivity in the accumulation of radioactivity in melanoma versus nonmalignant adjacent tissue. After sectioning, the boundary between the malignant tissue and the skin was clearly visible by macroscopic examination, making staining unnecessary. The autoradiographs of tumor and skin confirmed selective accumulation of ^{111}In-DOTA-MSH_{oct} in the tumor and showed that the radiopeptide diffused uniformly throughout the malignant tissue. The liver autoradiographs showed virtually no accumulation of radioactivity, corroborating the biodistribution experiments. In kidney, radioactivity was observed only in the cortex. Coinjection of an excess of α-MSH dramatically decreased radioactivity uptake in tumor but not in renal cortex.

In a second set of experiments, melanoma metastases were generated in mice by intravenous inoculation of B16F1 cells. At sacrifice, metastases were found in lung and

TABLE 2
Tissue Distribution at 4, 24, and 48 Hours After Injection

Tissue	Hours after injection					
	4		24		48	
	DOTA-NDP-MSH	DOTA-MSH_{oct}	DOTA-NDP-MSH	DOTA-MSH_{oct}	DOTA-NDP-MSH	DOTA-MSH_{oct}
Blood	0.17 ± 0.02	0.03 ± 0.00*	0.03 ± 0.00	0.00 ± 0.00*	0.02 ± 0.00	0.00 ± 0.00*
Muscle	0.94 ± 0.07	0.03 ± 0.01*	0.22 ± 0.02	0.01 ± 0.00*	0.11 ± 0.01	0.01 ± 0.00*
Liver	0.47 ± 0.05	0.41 ± 0.02	0.40 ± 0.02	0.38 ± 0.02	0.30 ± 0.02	0.33 ± 0.02
Kidney	8.04 ± 0.52 (8.69)	13.5 ± 1.12† (21.7)	4.93 ± 0.30	6.56 ± 0.77	2.38 ± 0.18	4.89 ± 0.34‡
Spleen	0.60 ± 0.05	0.15 ± 0.01*	0.69 ± 0.03	0.14 ± 0.01*	0.61 ± 0.05	0.14 ± 0.01*
Lung	0.23 ± 0.03	0.10 ± 0.01‡	0.19 ± 0.04	0.04 ± 0.00*	0.17 ± 0.01	0.05 ± 0.00*
Small intestine	0.29 ± 0.02	0.11 ± 0.03†	0.33 ± 0.08	0.06 ± 0.01‡	0.35 ± 0.07	0.04 ± 0.00†
Heart	0.06 ± 0.01	0.03 ± 0.00*	0.04 ± 0.00	0.02 ± 0.00*	0.04 ± 0.01	0.02 ± 0.00
Bone	1.29 ± 0.06	0.08 ± 0.01*	1.07 ± 0.07	0.07 ± 0.00*	0.83 ± 0.04	0.08 ± 0.01*
Pancreas	0.15 ± 0.01	0.03 ± 0.00*	0.12 ± 0.01	0.02 ± 0.00*	0.12 ± 0.01	0.02 ± 0.00‡
Skin	0.94 ± 0.10	0.10 ± 0.02*	0.56 ± 0.05	0.06 ± 0.01*	0.44 ± 0.04	0.08 ± 0.01*
Stomach	0.41 ± 0.07	0.10 ± 0.02‡	0.38 ± 0.12	0.25 ± 0.04	0.15 ± 0.02	0.11 ± 0.01
Adrenal	ND	0.18 ± 0.04	ND	0.13 ± 0.01	ND	0.31 ± 0.10
Tumor	6.32 ± 0.16 (1.15)	4.31 ± 0.30† (0.45)	2.74 ± 0.00	1.17 ± 0.13*	1.20 ± 0.11	1.08 ± 0.18

*$P < 0.0001$ vs ^{111}In-DOTA-NDP-MSH.
†$P < 0.01$ vs ^{111}In-DOTA-NDP-MSH.
‡$P < 0.001$ vs ^{111}In-DOTA-NDP-MSH.
ND = not determined.
^{111}In-DOTA-MSH_{oct} or ^{111}In-DOTA-NDP-MSH was injected to melanoma-bearing mice, and tissue-associated radioactivity was measured 4, 24, and 48 h after injection. Results are expressed as %ID/g (mean ± SEM, $n = 4–8$). Value in parentheses indicates tissue uptake in presence of 50 μg α-MSH. Tumor uptake 4, 24, and 48 h after injection was independent of tumor size as indicated by absence of statistically significant linear relationship between tumor size and tumor uptake (slope of linear correlation curve = −0.104 and 0.028; R^2 = 0.08 and 0.09; $P = 0.24$ and 0.30 for ^{111}In-DOTA-MSH_{oct} and ^{111}In-DOTA-NDP-MSH, respectively).

occasionally in liver. As illustrated in Figure 4, all macroscopically identified metastases (amelanotic and melanotic lesions) in lung or liver sections could be imaged on autoradiographs, clearly demonstrating the potential of ^{111}In-DOTA-MSH_{oct} to diagnose metastatic melanoma. Thus, tissue autoradiography confirmed the favorable biodistribution profile of ^{111}In-DOTA-MSH_{oct} and further showed that it could diffuse within the tumoral tissue, as demonstrated by the homogeneous distribution of radioactivity in the melanoma.

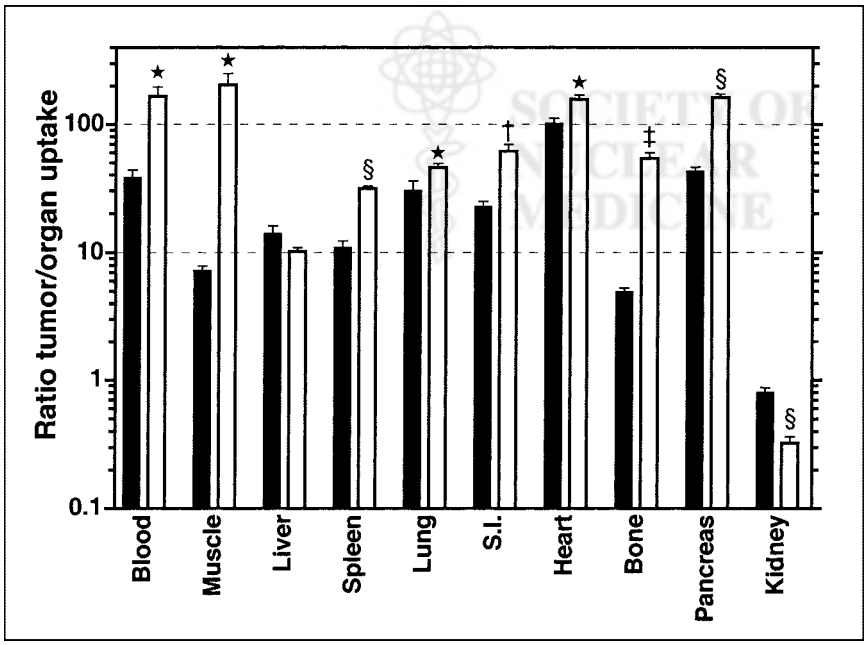

FIGURE 2. Tumor-to-organ uptake ratios 4 h after injection. ^{111}In-DOTA-MSH_{oct} (white bars) or ^{111}In-DOTA-NDP-MSH (black bars) was injected into melanoma-bearing mice, and tissues were collected 4 h after injection. Results are expressed as tumor-to-tissue uptake ratios (mean ± SEM, $n = 4–8$). *$P < 0.05$ vs. ^{111}In-DOTA-NDP-MSH. †$P < 0.01$ vs. ^{111}In-DOTA-NDP-MSH. ‡$P < 0.001$ vs. ^{111}In-DOTA-NDP-MSH. §$P < 0.0001$ vs. ^{111}In-DOTA-NDP-MSH.

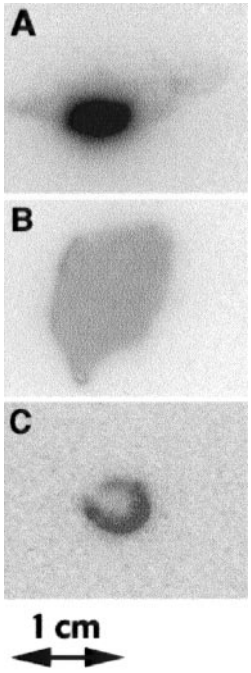

FIGURE 3. Autoradiographs of tissue sections from nonmalignant organs and primary melanoma: melanoma with surrounding skin tissue (A), liver (B), and transverse section of kidney (C). ^{111}In-DOTA-MSH$_{oct}$ was injected into melanoma-bearing mice, and tissues of interest were collected 4 h after injection and immediately fixed. After sectioning, tissues were exposed to storage phosphor plate. Similar autoradiographs were obtained for 3 mice.

Stability of ^{111}In-DOTA-MSH$_{oct}$ and ^{111}In-DOTA-NDP-MSH After Kidney Excretion

Urine samples were collected from melanoma-bearing mice previously injected with ^{111}In-DOTA peptide to assess in which form the radioligand was excreted. RP-HPLC analysis revealed that, 4 h after injection, most ^{111}In-DOTA-MSH$_{oct}$ was recovered intact in the urine. However, at 24 h after injection, the peak corresponding to ^{111}In-DOTA-MSH$_{oct}$ (elution time, 15.9 min) was not detectable and 2 radioactive metabolites were present: The major one (75% of total radioactivity) was eluted at 4.1 min, and the minor one was eluted at 8.9 min (Fig. 5). In contrast, no intact ^{111}In-DOTA-NDP-MSH was recovered in urine collected 4 h after injection. Thus, ^{111}In-DOTA-MSH$_{oct}$, but not ^{111}In-DOTA-NDP-MSH, exhibits good in vivo stability because it is excreted intact as late as 4 h after injection. Metabolites were detected when urine was collected after 24 h.

DISCUSSION

The goal of this project was to develop a radiolabeled α-MSH analog suitable for imaging MC1R-positive tumors, that is, melanoma, in patients. Therefore, on the basis of the results of our structure-affinity studies on α-MSH and the studies of others (reviewed in (*8*)), we synthesized a novel α-MSH analog (MSH$_{oct}$) and tested its in vitro and in vivo properties after coupling it to the metal chelator DOTA. This analog was shorter than the natural peptide and the superpotent α-MSH analog, NDP-MSH, to favor blood clearance. The full-length α-MSH analog, NDP-MSH, was also coupled to DOTA and used for comparison. Competition binding experiments with melanoma B16F1 cells revealed that DOTA-MSH$_{oct}$ retains high affinity for MC1R in the low-nanomolar range and full biologic activity as measured in a melanin bioassay. In addition, when radiolabeled with ^{111}In and injected into melanoma-bearing mice, DOTA-MSH$_{oct}$ exhibited an excellent biodistribution profile with regard to its potential use as a melanoma-targeting agent. Indeed, ^{111}In-DOTA-MSH$_{oct}$ was rapidly cleared from blood through the kidneys and, most important, accumulated preferentially in melanoma tissue: Four hours after injection, the melanoma-associated radioactivity was as much as 10–200 times greater than the radioactivity recovered in all nontarget organs with the exception of the kid-

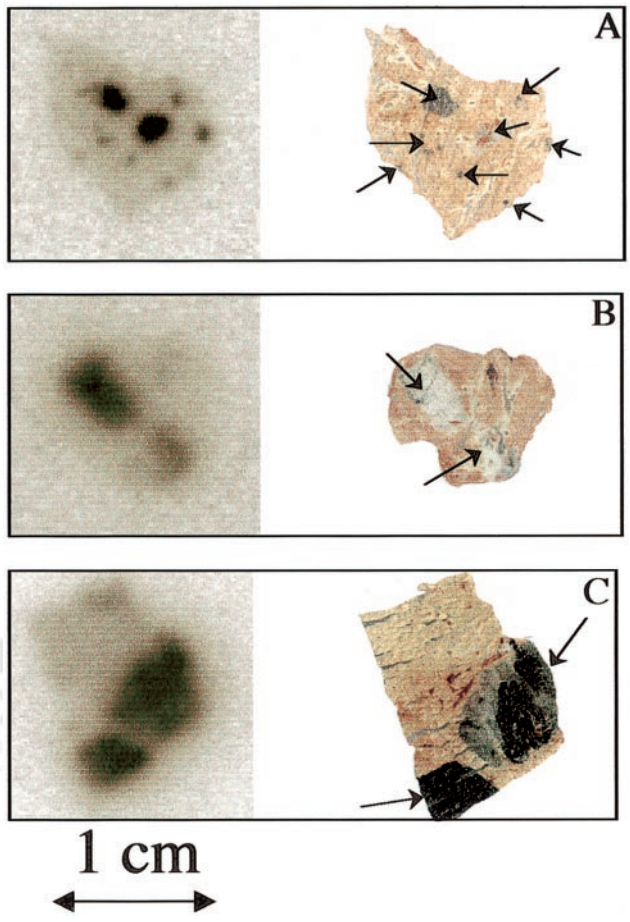

FIGURE 4. Autoradiographs of tissue sections from lung and liver colonized by melanoma metastases: lung with melanotic melanoma metastases (A), lung with amelanotic melanoma metastases (B), liver with melanotic melanoma metastases (C). ^{111}In-DOTA-MSH$_{oct}$ was injected into mice inoculated with B16F1 cells, and tissues showing macroscopic metastases were collected 4 h after injection and immediately fixed. After sectioning, tissues were exposed to storage phosphor plate (left) and later to scanner (right). Arrows indicate amelanotic/melanotic metastatic nodules.

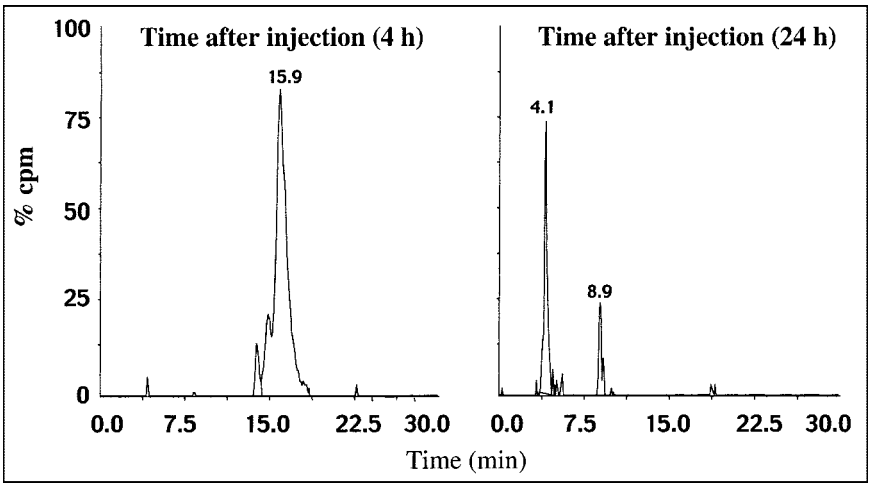

FIGURE 5. Radio-RP-HPLC analysis of urine samples 4 or 24 h after injection of ^{111}In-DOTA-MSH$_{oct}$. Urine samples were collected from melanoma-bearing mice (n = 4) and were analyzed by RP-HPLC after protein precipitation. Elution time of intact ^{111}In-DOTA-MSH$_{oct}$ was 15.9 min.

neys. The high tumor-to-liver and tumor-to-lung uptake ratios are of particular interest with regard to the prevalence of pulmonary and liver metastases in cutaneous melanoma patients (*9*). In accordance with the biodistribution experiment data, liver and lung metastases could easily be visualized on tissue autoradiographs. The results of ^{111}In-DOTA-MSH$_{oct}$ biodistribution, taken together with the results of a study showing that all melanotic and amelanotic melanoma cell lines express receptors for α-MSH (*19*), make this DOTA-α-MSH analog promising for melanoma diagnosis.

A comparative study with ^{111}In-DOTA-NDP-MSH clearly indicated the superiority of ^{111}In-DOTA-MSH$_{oct}$. ^{111}In-DOTA-NDP-MSH exhibited slower blood clearance together with much higher retention in organs widely distributed in the body, such as muscle, bone, and skin, or sensitive to radiation, such as bone, reducing both the diagnostic and the therapeutic potential. Whether intact ^{111}In-DOTA-NDP-MSH or a breakdown product accumulated in these nontarget organs is not clear, because in contrast to ^{111}In-DOTA-MSH$_{oct}$, ^{111}In-DOTA-NDP-MSH was shown to be unstable in vivo by the absence of intact peptide in urine 4 h after injection. Recently, Chen et al. (*20*) reported the biodistribution profile in melanoma-bearing mice of several ^{111}In-DOTA-α-MSH analogs, including ^{111}In-DOTA-NDP-MSH and a series of promising ^{111}In-DOTA-cyclic peptides. However, their uptake in skin and in the most radiosensitive organ, bone (*21*), was not given, making it difficult to compare their potential for melanoma diagnosis and receptor-mediated targeted radionuclide therapy.

Both biodistribution and autoradiography experiments indicate some kidney retention of ^{111}In-DOTA-MSH$_{oct}$ and ^{111}In-DOTA-NDP-MSH. This retention was found to be independent of the presence of α-MSH receptors because it could not be blocked by coadministration of an excess of cold ligand. On kidney autoradiographs, the radioactivity clearly appears to be concentrated mostly in the renal cortex, suggesting that ^{111}In-DOTA-MSH$_{oct}$ is retained in the proximal tubules probably after tubular reabsorption. Overall, the process of kidney accumulation of ^{111}In-DOTA-MSH$_{oct}$ strongly resembled that reported for other radiopeptides (*14*,*22*), suggesting a common mechanism of kidney uptake and retention. Therefore, one can assume that the pharmaceuticals known to lower nonspecific renal uptake of radiopeptides in patients (*23*) will be equally efficient for ^{111}In-DOTA-MSH$_{oct}$, making possible the use of this radioligand also for scintigraphic detection of melanoma metastases near the kidney.

Another exciting application of radiopeptides is internal radiotherapy. The present study showed that ^{111}In-DOTA-MSH$_{oct}$ accumulates specifically and, as evidenced on autoradiographs, homogeneously in the melanoma lesion. Moreover, preliminary internalization experiments revealed that ^{111}In-DOTA-MSH$_{oct}$ is highly internalized by isolated B16F1 cells after interaction with its receptor, thus offering the advantage of lowering the distance between the radiation emitter and the target nucleus and thereby maximizing radiation efficiency. These observations, together with the aptitude of DOTA to form stable complexes with various radiometals (*12*,*24*–*26*), including those exhibiting suitable physical characteristics for consideration as potential therapeutic radionuclides (e.g., ^{90}Y, ^{67}Ga, or even ^{111}In (*27*,*28*)), indicate that DOTA-MSH$_{oct}$ may be considered for radiotherapy if kidney accretion is reduced by administration of basic amino acids.

CONCLUSION

^{111}In-DOTA-MSH$_{oct}$ exhibits a more favorable overall performance than does ^{111}In-DOTA-NDP-MSH in murine models of primary and metastatic melanoma and thus is a promising melanoma imaging agent and a potential lead compound for radiotherapy of metastatic melanoma.

ACKNOWLEDGMENTS

We thank Prof. Helmut R. Mäcke (Department of Nuclear Medicine, Kantonsspital Basel) and his team for their assistance with the labeling experiments, Dr. Joyce Bau-

mann for her critical review of the manuscript, and Anne-Marie Meier for her excellent technical assistance. This work was supported by the Swiss Cancer League and the Roche Research Foundation.

REFERENCES

1. Dennis LK. Analysis of the melanoma epidemic, both apparent and real: data from the 1973 through 1994 surveillance, epidemiology, and end results program registry. *Arch Dermatol.* 1999;135:275–280.
2. Marchitto KS, Kindsvogel WR, Beaumier PL, et al. Characterization of a human-mouse chimeric antibody reactive with a human melanoma associated antigen. *Prog Clin Biol Res.* 1989;288:101–105.
3. Beaumier PL, Krohn KA, Carrasquillo JA, et al. Melanoma localization in nude mice with monoclonal Fab against p97. *J Nucl Med.* 1985;26:1172–1179.
4. Salk D. Technetium-labeled monoclonal antibodies for imaging metastatic melanoma: results of a multicenter clinical study. *Semin Oncol*. 1988;15:608–618.
5. Taylor A Jr, Milton W, Eyre HP, et al. Radioimmunodetection of human melanoma with indium-111-labeled monoclonal antibody. *J Nucl Med.* 1988;29: 329–337.
6. Mars U, Larsson BS. Thiourea as a melanoma targeting agent. *Melanoma Res.* 1996;6:113–120.
7. Krenning EP, Kwekkeboom DJ, Bakker WH, et al. Somatostatin receptor scintigraphy with [^{111}In-DTPA-D-Phe1]- and [^{123}I-Tyr^3]-octreotide: the Rotterdam experience with more than 100 patients. *Eur J Nucl Med.* 1993;20:716–731.
8. Eberle AN. Proopiomelanocortin and the melanocortin peptides. In: Cone RD, eds. *The Melanocortin Receptors.* Totowa, NJ: Humana Press Inc.; 2000:3–67.
9. Balch CM, Soong SJ, Murad TM, Smith JW, Maddox WA, Durant JR. A multifactorial analysis of melanoma. IV. Prognostic factors in 200 melanoma patients with distant metastases (stage III). *J Clin Oncol.* 1983;1:126–134.
10. Chen J, Cheng Z, Hoffman TJ, Jurisson SS, Quinn TP. Melanoma-targeting properties of ^{99m}technetium-labeled cyclic alpha-melanocyte-stimulating hormone peptide analogues. *Cancer Res.* 2000;60:5649–5658.
11. Cutler CS, Smith CJ, Ehrhardt GJ, Tyler TT, Jurisson SS, Deutsch E. Current and potential therapeutic uses of lanthanide radioisotopes. *Cancer Biother Radiopharm.* 2000;15:531–545.
12. Kozak RW, Raubitschek A, Mirzadeh S, et al. Nature of the bifunctional chelating agent used for radioimmunotherapy with yttrium-90 monoclonal antibodies: critical factors in determining in vivo survival and organ toxicity. *Cancer Res.* 1989;49:2639–2644.
13. De Jong M, Bakker WH, Breeman WA, et al. Pre-clinical comparison of [DTPA^0] octreotide, [DTPA^0, Tyr^3] octreotide and [DOTA^0, Tyr^3] octreotide as carriers for somatostatin receptor-targeted scintigraphy and radionuclide therapy. *Int J Cancer.* 1998;75:406–411.
14. Froidevaux S, Heppeler A, Eberle AN, et al. Preclinical comparison in AR4-2J tumor bearing mice of four radiolabeled DOTA-somatostatin analogs for tumor diagnosis and internal radiotherapy. *Endocrinology.* 2000;141:3304–3312.
15. Otte A, Herrmann R, Heppeler A, et al. Yttrium-90 DOTATOC: first clinical results. *Eur J Nucl Med.* 1999;26:1439–1447.
16. Heppeler A, Froidevaux S, Mäcke HR, et al. Radiometal labelled macrocyclic chelator derivatised somatostatin analogue with superb tumour targeting properties and potential for receptor mediated internal radiotherapy. *Chem Eur J.* 1999;5:1016–1023.
17. Siegrist W, Solca F, Stutz S, et al. Characterization of receptors for alpha-melanocyte-stimulating hormone on human melanoma cells. *Cancer Res.* 1989; 49:6352–6358.
18. Fidler IJ. Selection of successive tumour lines for metastasis. *Nat New Biol.* 1973;242:148–149.
19. Jiang J, Sharma SD, Fink JL, Hadley ME, Hruby VJ. Melanotropic peptide receptors: membrane markers of human melanoma cells. *Exp Dermatol.* 1996;5: 325–333.
20. Chen J, Cheng Z, Owen NK, et al. Evaluation of an ^{111}In-DOTA-rhenium cyclized alpha-MSH analog: a novel cyclic-peptide analog with improved tumor-targeting properties. *J Nucl Med.* 2001;42:1847–1855.
21. Fawwaz RA, Wang TS, Srivastava SC, Hardy MA. The use of radionuclides for tumor therapy. *Int J Rad Appl Instrum B.* 1986;13:429–436.
22. Duncan JR, Stephenson MT, Wu HP, Anderson CJ. Indium-111-diethylenetriaminepentaacetic acid-octreotide is delivered in vivo to pancreatic, tumor cell, renal, and hepatocyte lysosomes. *Cancer Res.* 1997;57:659–671.
23. Hammond PJ, Wade AF, Gwilliam ME, et al. Amino acid infusion blocks renal tubular uptake of an indium-labelled somatostatin analogue. *Br J Cancer.* 1993; 67:1437–1439.
24. Deshpande SV, DeNardo SJ, Kubis DL, et al. Yttrium-90-labeled antibody for therapy: labeling by a new macrocyclic bifunctional chelating agent. *J Nucl Med.* 1990;31:473–479.
25. Camera L, Kinuya S, Garmestani K, et al. Evaluation of the serum stability and in vivo biodistribution of CHX-DTPA and other ligands for yttrium labeling of monoclonal antibodies. *J Nucl Med.* 1994;35:882–889.
26. Chinol M, Paganelli G, Sudati F, Meares C, Fazio F. Biodistribution in tumour-bearing mice of two ^{90}Y-labelled biotins using three-step tumour targeting. *Nucl Med Commun.* 1997;18:176–182.
27. Griffiths GL, Govindan SV, Sgouros G, Ong GL, Goldenberg DM, Mattes MJ. Cytotoxicity with Auger electron-emitting radionuclides delivered by antibodies. *Int J Cancer.* 1999;81:985–992.
28. Krenning EP, Kooij PPM, Bakker WH, et al. Radiotherapy with a radiolabeled somatostatin analogue, [^{111}In-DTPA-D-Phe^1]-octreotide: a case history. *Ann NY Acad Sci.* 1994;733:496–506.